R & M. No. 3366

MINISTRY OF AVIATION

AERONAUTICAL RESEARCH COUNCIL
REPORTS AND MEMORANDA

The Buckling Strength of a Uniform Circular Cylinder Loaded in Axial Compression

By A. J. Sobey

LONDON: HER MAJESTY'S STATIONERY OFFICE
1964
PRICE 9*s.* 6*d.* NET

The Buckling Strength of a Uniform Circular Cylinder Loaded in Axial Compression

By A. J. Sobey

Communicated by the Deputy Controller Aircraft (Research and Development), Ministry of Aviation

*Reports and Memoranda No. 3366**

August, 1962

Summary.

The theoretical estimation of the buckling strength of a cylinder loaded in axial compression is improved by the use of a more representative deflected form for the buckled cylinder than has previously been used. Kempner's buckling strength for dead-weight loading is reduced by 18%. The presentation of the magnitude and distribution of the constraint system required to maintain the mode is novel and instructive.

LIST OF CONTENTS

* Replaces R.A.E. Report No. Structures 279—A.R.C. 24 503.

LIST OF TABLES

LIST OF ILLUSTRATIONS

---

1. *Introduction.*

The failure of theoretical investigations to predict the observed buckling strength of cylinders loaded in axial compression has been discussed extensively in the literature[1 to 4]. The measured values are significantly less than the best available estimates (Kempner[4]). Various attempts to explain away the discrepancy have been propounded, but none is wholly satisfactory.

The theoretical investigations available follow a well-defined pattern, due to Karman and Tsien[1]. The stress-strain, the compatibility conditions and the equilibrium of stress in the tangent plane are all satisfied but the equation of radial equilibrium is left unsatisfied and is replaced by an energy criterion. If the radial-equilibrium condition were to be satisfied by any solution based on a tentative mode for the deflected shape of the cylinder, an exact solution of the large-deflection analysis would have been found. Disequilibrium in the radial direction results in a stress-strain characteristic in which the mean axial stress, for any given mean axial strain, is necessarily high for all cases of stable equilibrium. The buckling conditions estimated on this basis are optimistic.

If a simple expression for the mode of deformation of the cylinder is selected, it is unreasonable to expect that the stresses in the immediate post-buckled region (up to mean axial strains of the order of $1{\cdot}5t/R$) will be accurate estimates of the unknown solution of the von Karman large-deflection equations for the cylinder. Previous investigators[1 to 4] have chosen modes for the

deformed state of the cylinder which have been assumed satisfactory on the basis of the observed extreme patterns of post-buckling behaviour. However, as will be seen below, such simplified modes cannot be justified in the region of minimum post-buckled stress.

A simple mode of the type used by previous workers in the field[1 to 4] includes, as extreme patterns of deflection, the chessboard type[5] of buckling associated with small-deflection theory and which is known to be valid in the immediate neighbourhood of the small-deflection buckling region. For large strain, that is for the fully developed post-buckled state, a polyhedral form with diamond nodal lines is observed, and this nodal pattern is included in the assumed mode. However, a superposition of this diamond type of buckling on the chessboard type may not be satisfactory in the transitional region between these two extremes. It is in this region that errors in stress estimation will be most serious.

The linear theory assumes a mode which comprises a uniform inward displacement together with a single periodic function of the co-ordinates (x, y). The first perturbation of this solution contains four additional terms[4] whose periodicities are respectively (0, 2) (2, 0) (1, 3) and (3, 1) in the x and y directions. The latter two terms have always been discarded, but, as will be shown below, they are important in the critical post-buckled region referred to above. By their inclusion, reductions in mean axial stress for a given mean axial strain in that region of the order of 18 to 25 per cent are realised, with comparable reductions in the buckling strength.

In addition to the inclusion of the two terms previously discarded, the analysis given below examines the constraint system necessary to maintain the assumed mode. This takes the form of a pressure distribution over the cylindrical surface which varies from place to place. With a knowledge of this constraint system, those parts of the buckle pattern which are being pushed in (or forced out) can be seen to be deflecting too little (or too much) and a more realistic impression of the optimum mode is established. The influence of the constraint pressures diminishes as their frequency increases, and it is found that the pressure components corresponding to Kempner's omitted terms are two of the most important ones.

The reduction in buckling strength indicated by this extension of previous work is more consistent with experimental data. A direct comparison with experiment is, however, beyond the scope of this paper, and it is intended only that this investigation should provide a more realistic theoretical estimate for the ideal structural element under ideal loading conditions than has been available hitherto.

2. *Buckling Criteria.*

The form of the stress-strain characteristic for the cylinder in the pre- and post-buckled conditions is illustrated in Fig. 2a. The portion OA corresponds to the uniform compression without deflection of the pre-buckled condition. The curve AE is appropriate to the deformed state of the cylinder.

Tsien[6] has shown how buckling criteria for the shell can be based on energy considerations. If the cylinder is compressed in a rigid-test machine the pressure is applied over the ends of the cylinder in such a manner that on buckling there is no loss of energy from the machine. The cylinder may buckle, therefore, when the strain energy absorbed from the test machine by the cylinder has the same value in the undeflected and deflected states.

Fig. 2b shows the energy distribution in the cylinder for the various parts of the stress-strain characteristic. The figure has been drawn with a base of $(e)^2$ so as to linearize the energy in the pre-buckled state, (OA). From A to the minimum post-buckled strain, the load is decreasing and the

cylinder releases energy, so that the system is unstable. From C to E the cylinder increases in energy with increase in strain until it reaches a point B_2 at which the energy is equal to the value reached at the point A_2 on loading up from O to A. Further increase in strain leads to a rise in strain energy. Thus for the entire cycle, the cylinder is in stable equilibrium from O to A_2 and from B_2 onward. Between A_2 and A, A and C, C and B_2 it is unstable provided that the cylinder can freely take up the mode of deformation. Otherwise the region A_2 to A is a meta-stable state and the cylinder will require a disturbance to produce buckling before A is reached. In practice there is always a source of extraneous energy present in which case the cylinder may not be loaded beyond A_2 without buckling. The cylinder can only buckle before it reaches A_2 if there is a surplus of energy absorbed by the cylinder. It is reasonable to postulate that the cylinder, once it reaches a point X on the characteristic CB_2, will stay buckled. It can buckle at a point X_1 before A_2 only if the energy 'jump' X_1X is spontaneously available from outside the test machine. This, in theory, can happen, so that at any point on OA between C_1 and A_2 buckling might occur.

X_1 should, in practice, be close to A_2, for the energy involved in effecting the jump X_1 to X is not small. To jump from C_1 to C requires a proportional increase in stored energy of the order of 20%. This is unlikely to be available in practice. Nevertheless C_1 will be designated the lower limit of buckling strain for rigid-loading-machine conditions while A_2 is the corresponding upper limit. The theoretically possible meta-stable region A_2A is discounted, on the assumption that all modes are equally likely and that the cylinder has a preference for a mode with least possible strain energy.

Corresponding to the upper and lower buckling strains for rigid-test-machine conditions, upper and lower buckling stresses can be established for dead-weight loading. Fig. 2c shows how the variation with $(\text{stress})^2$ of the total potential energy—that is of the strain energy stored in the cylinder less the potential energy of the weight. From O to A, total potential energy falls, linearly with $(\sigma)^2$. From A to D, the cylinder unloads and is unstable. From D onward the cylinder begins to lose total potential energy (i.e. positive stiffness) until at B_1 the total potential energy is equal in the deflected condition to what it was at the point A_1 on loading up, and the cylinder stabilises. Thereafter total potential energy diminishes faster in the buckled shape than in the pre-buckled condition. A_1 is the upper limit of buckling stress, meta-stable states again being rejected. Since it is theoretically possible for jumps to occur from characteristic OA_1 to DB_1, the cylinder can buckle at values of σ intermediate between D_1 and A_1. D_1 is the 'lower limit of buckling stress for dead-weight loading'.

All practical tests are conducted on test machines with a finite rigidity. The extreme conditions of infinite spring stiffness and zero spring stiffness are the rigid-test-machine and dead-weight-loading conditions respectively. All finite rigidity conditions are intermediate between the extremes and upper and lower limits on buckling for this case can be formed in the same manner as above, for dead-weight loading if the total-potential-energy function includes the energy stored in the spring or test machine. A_3B_3 (Fig. 2d) is representative of such a condition. When the cylinder reaches A_3, by simultaneous application of stress and strain, it may unload to B_3 along a line whose negative slope is the spring stiffness of the test machine. Fig. 2d shows the total-potential-energy diagram for this case. The cylinder loads up to A, unloads from A to a point G which is the point on AE where the slope is negatively equal to the spring stiffness. Thereafter the system has positive stiffness and becomes stable again at B_3 whereafter it continues to lose total potential energy along the characteristic B_3E. It is obvious that every such case is intermediate between the extremes of rigid-machine and dead-weight loading. Hereafter only these two conditions will be discussed.

The stability conditions are developed from calculations of the strain energy for a given applied strain. The stress associated with the given strain is calculated and the total potential energy determined. The two energy diagrams for the extreme loading conditions are then prepared, and the buckling strain and stress in the two cases are found.

3. *Analytical Development of Solution.*

3.1. *The General Conditions of Equilibrium and Compatibility.*

Equilibrium of the stresses in the tangent plane is assured if

$$\frac{\partial \sigma_x}{\partial x} + \frac{\partial \tau_{xy}}{\partial y} = \frac{\partial \sigma_y}{\partial y} + \frac{\partial \tau_{xy}}{\partial x} = 0 \tag{1}$$

which conditions are satisfied automatically by the introduction of the Airy stress function F, where

$$\sigma_x = \frac{\partial^2 F}{\partial y^2}, \quad \tau_{xy} = -\frac{\partial^2 F}{\partial x \partial y}, \quad \sigma_y = \frac{\partial^2 F}{\partial x^2}. \tag{2}$$

The strain-displacement relations for the large deflections considered are

$$\left.\begin{aligned} \epsilon_x &= \frac{\partial u}{\partial x} + \frac{1}{2}\left(\frac{\partial w}{\partial x}\right)^2 \\ \epsilon_y &= \frac{\partial v}{\partial y} + \frac{1}{2}\left(\frac{\partial w}{\partial y}\right)^2 - \frac{w}{R} \\ \gamma_{xy} &= \frac{\partial u}{\partial y} + \frac{\partial v}{\partial x} + \frac{\partial w}{\partial x}\frac{\partial w}{\partial y}. \end{aligned}\right\} \tag{3}$$

The equation of compatibility of strain is, therefore

$$\frac{\partial^2 \epsilon_x}{\partial y^2} + \frac{\partial^2 \epsilon_y}{\partial x^2} - \frac{\partial^2 \gamma_{xy}}{\partial x \partial y} = \left(\frac{\partial^2 w}{\partial x \partial y}\right)^2 - \frac{\partial^2 w}{\partial x^2}\frac{\partial^2 w}{\partial y^2} - \frac{1}{R}\frac{\partial^2 w}{\partial x^2}. \tag{4}$$

The stress-strain relations may be written

$$\left.\begin{aligned} E\epsilon_x &= \sigma_x - \nu\sigma_y \\ E\epsilon_y &= \sigma_y - \nu\sigma_x \\ E\gamma_{xy} &= 2(1+\nu)\tau_{xy} \end{aligned}\right\} \tag{5}$$

where E is Young's modulus, and ν is Poisson's ratio, which will be taken as $0 \cdot 3$.

Substituting from equation (5) into (4) and using equations (1), we get

$$\frac{1}{E}\left\{\frac{\partial^2 \sigma_x}{\partial y^2} + \frac{\partial^2 \sigma_y}{\partial x^2} - 2\frac{\partial^2 \tau_{xy}}{\partial x\, \partial y}\right\} = \left(\frac{\partial^2 w}{\partial x\, \partial y}\right)^2 - \frac{\partial^2 w}{\partial x^2}\frac{\partial^2 w}{\partial y^2} - \frac{1}{R}\frac{\partial^2 w}{\partial x^2}$$

or, on introducing F from equation (2), the equation of compatibility of strain in the tangent plane takes the form

$$\frac{1}{E}\nabla^4 F = \left\{\left(\frac{\partial^2 w}{\partial x\, \partial y}\right)^2 - \frac{\partial^2 w}{\partial x^2}\frac{\partial^2 w}{\partial y^2}\right\} - \frac{1}{R}\frac{\partial^2 w}{\partial x^2}. \tag{6}$$

The equation of radial equilibrium is

$$D\nabla^4 w = p + \frac{\partial}{\partial x}\left(t\sigma_x \frac{\partial w}{\partial x}\right) + \frac{\partial}{\partial y}\left(t\tau_{xy} \frac{\partial w}{\partial x}\right) + \frac{\partial}{\partial x}\left(t\tau_{xy} \frac{\partial w}{\partial y}\right) + \\ + \frac{\partial}{\partial y}\left(t\sigma_y \frac{\partial w}{\partial y}\right) + \frac{t}{R}\sigma_y \tag{7}$$

where p is measured positively in the z direction ($p > 0$ means external pressure) which, on using equations (1) and substituting from equation (2) gives

$$D\nabla^4 w = p + \frac{t}{R}\frac{\partial^2 F}{\partial x^2} + t\left\{\frac{\partial^2 F}{\partial y^2}\frac{\partial^2 w}{\partial x^2} - 2\frac{\partial^2 F}{\partial x\,\partial y}\frac{\partial^2 w}{\partial x\,\partial y} + \frac{\partial^2 F}{\partial x^2}\frac{\partial^2 w}{\partial y^2}\right\}. \tag{8}$$

Equations (6) and (8) are the von Karman large-deflection equations for the circular cylinder.

3.2. *Development of Solution for Assumed Modes $w(x, y)$.*

For any specified conditions of loading, we seek simultaneous solutions w and F of equations (6) and (8). In practice this is not feasible and equation (8) is abandoned in favour of a minimum-energy criterion which, for free variation of w, is formally equivalent to equation (8). Given any tentative approximation to w, the choice of its parameters will be based on an energy criterion.

The linear solution of the cylinder problem has been known for some time[4], and is obtained by omitting the terms in { } occurring in equations (6) and (8). This solution is

$$w = w_1\{\cos(\pi x/\lambda_x)\cos(\pi y/\lambda_y)\} + w_2. \tag{9}$$

If, now, this solution is substituted into the right-hand side of equation (6), the first correction to F is found, and on substituting this improved estimate of F into equation (8), with zero pressure p, a better approximation to w is derived.

This takes the form

$$w = \xi t\{\cos(\pi x/\lambda_x)\cos(\pi y/\lambda_y) + \alpha\cos(2\pi x/\lambda_x) + \beta\cos(2\pi y/\lambda_y) + \\ + \gamma\cos(\pi x/\lambda_x)\cos(3\pi y/\lambda_y) + \delta\cos(3\pi x/\lambda_x)\cos(\pi y/\lambda_y) + \epsilon\}. \tag{10}$$

In previous solutions of this problem Karman and Tsien took $\alpha = \beta$, and $\gamma = \delta = 0$; which practice was followed by Leggett and Jones[2], and by Michielsen[3]. Kempner[4] retained $\gamma = \delta = 0$ but allowed α and β to vary freely.

The representation (10) of w is taken as appropriate for determining the post-buckled characteristic of the cylinder.

On substituting from equation (10) into equation (6) and integrating the resulting equation, the following form for F is obtained:

$$F = -(Et^2/\mu^2\eta^2)\sum\sum f_{mn}\cos(m\pi x/\lambda_x)\cos(n\pi y/\lambda_y) - \sigma y^2/2 \tag{11}$$

where

σ is the average applied end compressive stress,

$\mu = \lambda_y/\lambda_x$,

$\eta = \pi^2 Rt/\lambda_y^2$,

$\omega = \xi\eta$

and the only non-zero f_{mn} are the following:

$$\left.\begin{aligned}
f_{02} &= \omega^2\mu^4[1+2\gamma+9\delta^2]/32\\
f_{04} &= \omega^2\mu^4\gamma/64\\
f_{06} &= \omega^2\mu^4\gamma^2/288\\
f_{11} &= \omega\mu^4[2\alpha\omega(1+\delta)+2\beta\omega(1+\gamma)-1]/(\mu^2+1)^2\\
f_{13} &= \omega\mu^4[2\beta\omega+18\alpha\gamma\omega-\gamma]/(\mu^2+9)^2\\
f_{15} &= 2\omega^2\mu^4\beta\gamma/(\mu^2+25)^2\\
f_{20} &= \omega[(1+9\gamma^2+2\delta)\omega-8\alpha]/32\\
f_{22} &= \omega^2\mu^4[4\alpha\beta+\gamma+4\gamma\delta+\delta]/4(\mu^2+1)^2\\
f_{24} &= \omega^2\mu^4\gamma(1+25\delta)/16(\mu^2+4)^2\\
f_{31} &= \omega\mu^4[2\alpha\omega+18\beta\delta\omega-9\delta]/(9\mu^2+1)^2\\
f_{33} &= 2\omega^2\mu^4(\alpha\gamma+\beta\delta)/9(\mu^2+1)^2\\
f_{40} &= \omega^2\delta/64\\
f_{42} &= \omega^2\mu^4\delta(1+25\gamma)/16(4\mu^2+1)^2\\
f_{44} &= \omega^2\mu^4\gamma\delta/16(\mu^2+1)^2\\
f_{51} &= 2\omega^2\mu^4\alpha\delta/(25\mu^2+1)^2\\
f_{60} &= \omega^2\delta^2/288\,.
\end{aligned}\right\} \qquad (12)$$

3.3. *Strain-Energy Functions.*

The strain energy due to bending is

$$\begin{aligned}
U_1 &= \tfrac{1}{2}D\int_0^L\int_0^{2\pi R}\left[(\nabla^2 w)^2+2(1-\nu)\left\{\left(\frac{\partial^2 w}{\partial x\,\partial y}\right)^2-\frac{\partial^2 w}{\partial x^2}\frac{\partial^2 w}{\partial y^2}\right\}\right]dx\,dy\\
&= \frac{\pi D\omega^2 L}{4R}[(1+\mu^2)^2+32\alpha^2\mu^4+32\beta^2+\gamma^2(\mu^2+9)^2+\delta^2(9\mu^2+1)^2]\,. \qquad (13)
\end{aligned}$$

The strain energy due to the extensional stresses is

$$U_2 = \frac{t}{2E}\int_0^L\int_0^{2\pi R}\left[(\nabla^2 F)^2+2(1+\nu)\left\{\left(\frac{\partial^2 F}{\partial x\,\partial y}\right)^2-\frac{\partial^2 F}{\partial x^2}\frac{\partial^2 F}{\partial y^2}\right\}\right]dx\,dy\,.$$

On introducing the non-dimensional stress $\sigma^* = \sigma R/Et$ and combining U_1, U_2, the total strain energy is

$$\begin{aligned}
U = U_1+U_2 = (\pi LEt^3/R)\Bigg[&\frac{\omega^2}{48(1-\nu^2)}\{(1+\mu^2)^2+32\alpha^2\mu^4+32\beta^2+\gamma^2(\mu^2+9)^2+\delta^2(9\mu^2+1)^2\}+\\
&+(\sigma^*)^2+(\omega^4\mu^4/128\eta^2)\{(1+2\gamma+9\delta^2)^2+4\gamma^2+\gamma^4\}+\\
&+(\omega^2\mu^4/4(1+\mu^2)^2\eta^2)\{(2\alpha\omega[1+\delta]+2\beta\omega[1+\gamma]-1)^2+\omega^2(4\alpha\beta+\gamma+4\gamma\delta+\delta)^2+\\
&+4\omega^2(\alpha\gamma+\beta\delta)^2+\omega^2\gamma^2\delta^2\}+\\
&+(2\beta\omega+18\alpha\gamma\omega-\gamma)^2\omega^2\mu^4/4(\mu^2+9)^2\eta^2+(2\alpha\omega+18\beta\delta\omega-9\delta)^2\omega^2\mu^4/4(9\mu^2+1)^2\eta^2+\\
&+\beta^2\gamma^2\omega^4\mu^4/(\mu^2+25)^2\eta^2+\alpha^2\delta^2\omega^4\mu^4/(25\mu^2+1)^2\eta^2+\gamma^2(1+25\delta)^2\omega^4\mu^4/64(\mu^2+4)^2\eta^2+\\
&+\delta^2(1+25\gamma)^2\omega^4\mu^4/64(1+4\mu^2)^2\eta^2+(\omega^2/128\eta^2)\{[(1+9\gamma^2+2\delta)\omega-8\alpha]^2+4\delta^2\omega^2+\omega^2\delta^4\}\Bigg]\,. \qquad (14)
\end{aligned}$$

3.4. *Restrictions on the Variables.*

U is a function of $(\sigma^*, \alpha, \beta, \gamma, \delta, \omega, \eta, \mu)$ but these eight parameters are not independent.

The mean radial contraction of the cylinder is determined from the continuity condition for v displacements $\int_0^L \int_0^{2\pi R} \frac{\partial v}{\partial y}\, dy\, dx = 0$ which gives

$$\xi\epsilon = (\omega^2/8\eta)(1+8\beta^2+9\gamma^2+\delta^2) - \nu\sigma^*. \tag{15}$$

The mean axial strain $e = -\frac{1}{2\pi LR}\int_0^L \int_0^{2\pi R} \frac{\partial u}{dx}\, dx\, dy = e^* t/R$ say, where e^* is a reduced unit of strain and on substituting and simplifying, we obtain

$$e^* = \sigma^* + (\mu^2\omega^2/8\eta)(1+8\alpha^2+\gamma^2+9\delta^2). \tag{16}$$

3.5. *Choice of Parameters.*

If the cylinder is loaded by strain increments as in a rigid-test machine, U has to be minimised for a given e^* subject to the constraint (16).

If we have dead-weight loading, the total energy of the system must include the potential energy of the (moving) applied load σ, which has the value

$$W = \int_0^{2\pi R} \int_0^L t\sigma_x \frac{\partial u}{\partial x}\, dy\, dx = (\pi E t^3 L/R)(2\sigma^* e^*) \tag{17}$$

and the parameters are determined from the condition that the total potential energy $U - W$ is to be a minimum.

For either of these problems, the choice of parameters is resolved by using a direct minimization procedure on a digital computer. The programme used in this paper is due to Rosenbrock[7].

For rigid-machine-loading conditions U is minimised for a given e^* and the mean axial applied stress σ^* which reacts against the machine is deduced. The appropriate post-buckled stress-strain relation for this loading is found.

Similarly for dead-weight loading $U - W$ is minimised for a given σ^* and the mean axial strain e^* which is developed under the load is deduced. The appropriate post-buckling stress-strain curve for dead-weight loading is obtained and coincides with the stress-strain characteristic for rigid-machine loading.

If σ^*, e^* are values of mean axial applied stress and strain which correspond to a point of this characteristic, then the set of parameters $\alpha, \beta, \gamma, \delta, \omega, \eta, \mu$ which are optimal for e^* in the first problem is identical with the set which is optimal for σ^* in the second.

For optimal choice of parameters the energy variation (U) in the first problem is shown as a function of $(e^*)^2$ in Fig. 3 and the total potential energy $(U-W)$ in the second as a function of $(\sigma^*)^2$ in Fig. 4. The mode shape appropriate to the optimum solution of the first problem for a post-buckled strain $e^* = 1$ is shown in Fig. 5. The modal parameters $\alpha, \beta, \gamma, \delta, \omega, \eta$ and μ^2 are plotted against σ^* in Fig. 6 and show the smooth transition through the region of minimum post-buckled stress which suggests that the approximation of equation (10) is valid.

The post-buckled stress-strain curve for the cylinder is shown in Fig. 7, with an indication in broken line of that portion of the characteristic which has not been computed which corresponds in either problem to unstable equilibrium.

4. *The Effect of Equilibrating Pressures.*

The approximate solution to the formal problem is an exact solution of an allied problem, namely that of a cylinder which carries loads not only over its ends, but over the curved surface as well. For the assumed mode of equation (10) and the Airy stress function derived from equation (11), equation (8) is satisfied if, and only if, there exists a pressure distribution over the curved surface, whose value is given by substituting for w and F into equation (8). This pressure is referred to as the constraint pressure, p. Work is done on the cylinder by the pressure system p, which acts over the displacement w of equation (10), and does the quantity of work

$$\overline{W} = \int_0^{2\pi R} \int_0^L pw \, dy \, dx . \tag{18}$$

Substituting from equations (10), (11) into equation (8) we find that

$$\begin{aligned}
pR^2/Et^2 = {} & (\omega\eta/12(1-\nu^2))\{(\mu^2+1)^2 \cos(\pi x/\lambda_x)\cos(\pi y/\lambda_y) + 16\alpha\mu^4 \cos(2\pi x/\lambda_x) + \\
& + 16\beta \cos(2\pi y/\lambda_y) + \gamma(\mu^2+9)^2 \cos(\pi x/\lambda_x)\cos(3\pi y/\lambda_y) + \\
& + \delta(9\mu^2+1)^2 \cos(3\pi x/\lambda_x)\cos(\pi y/\lambda_y)\} - \\
& - \frac{1}{\eta} \sum\sum m^2 f_{mn} \cos(m\pi x/\lambda_x)\cos(n\pi y/\lambda_y) - \\
& - \mu^2\omega\sigma^*\{\cos(\pi x/\lambda_x)\cos(\pi y/\lambda_y) + 4\alpha\cos(2\pi x/\lambda_x) + \\
& + \gamma\cos(\pi x/\lambda_x)\cos(3\pi y/\lambda_y) + 9\delta\cos(3\pi x/\lambda_x)\cos(\pi y/\lambda_y)\} + \\
& + \frac{\omega}{4\eta} \sum\sum [(m+n)^2\{\cos[(m+1)\pi x/\lambda_x]\cos[(n-1)\pi y/\lambda_y] + \\
& + \cos[(m-1)\pi x/\lambda_x]\cos[(n+1)\pi y/\lambda_y]\} + \\
& + (m-n)^2\{\cos[(m+1)\pi x/\lambda_x]\cos[(n+1)\pi y/\lambda_y] + \\
& + \cos[(m-1)\pi x/\lambda_x]\cos[(n-1)\pi y/\lambda_y]\}]f_{mn} + \\
& + \frac{2\alpha\omega}{\eta} \sum\sum n^2\{\cos[(m+2)\pi x/\lambda_x] + \cos[(m-2)\pi x/\lambda_x]\}\cos(n\pi y/\lambda_y) f_{mn} + \\
& + \frac{2\beta\omega}{\eta} \sum\sum m^2\cos(m\pi x/\lambda_x)\{\cos[(n+2)\pi y/\lambda_y] + \cos[(n-2)\pi y/\lambda_y]\} f_{mn} + \\
& + \frac{\gamma\omega}{4\eta} \sum\sum [(3m+n)^2\{\cos[(m+1)\pi x/\lambda_x]\cos[(n-3)\pi y/\lambda_y] + \\
& + \cos[(m-1)\pi x/\lambda_x]\cos[(n+3)\pi y/\lambda_y]\} + \\
& + (3m-n)^2\{\cos[(m+1)\pi x/\lambda_x]\cos[(n+3)\pi y/\lambda_y] + \\
& + \cos[(m-1)\pi x/\lambda_x]\cos[(n-3)\pi y/\lambda_y]\}]f_{mn} + \\
& + \frac{\delta\omega}{\eta} \sum\sum [(m+3n)^2\{\cos[(m+3)\pi x/\lambda_x]\cos[(n-1)\pi y/\lambda_y] + \\
& + \cos[(m-3)\pi x/\lambda_x]\cos[(n+1)\pi y/\lambda_y]\} + \\
& + (m-3n)^2\{\cos[(m+3)\pi x/\lambda_x]\cos[(n+1)\pi y/\lambda_y] + \\
& + \cos[(m-3)\pi x/\lambda_x]\cos[(n-1)\pi y/\lambda_y]\}]f_{mn} .
\end{aligned} \tag{19}$$

This expression can be written

$$pR^2/Et^2 = p_{11}\cos(\pi x/\lambda_x)\cos(\pi y/\lambda_y) + p_{20}\cos(2\pi x/\lambda_x) + p_{02}\cos(2\pi y/\lambda_y) + \\ + p_{13}\cos(\pi x/\lambda_x)\cos(3\pi y/\lambda_y) + p_{31}\cos(3\pi x/\lambda_x)\cos(\pi y/\lambda_y), \tag{20}$$

plus thirty other terms which do no work over the displacement system of equation (10).

There is no mean pressure present.

The coefficients in p which do work over the displacement system w are

$$\left.\begin{aligned}
p_{11} &= \omega\eta(\mu^2+1)^2/12(1-\nu^2) - f_{11}/\eta - \mu^2\omega\sigma^* + \\
&\quad + \frac{\omega}{\eta}\{2(1+\gamma)f_{02} + 8\gamma f_{04} + 2(\alpha+\beta)f_{11} + 2\beta f_{13} + 2(1+\delta)f_{20} + 4(\gamma+\delta)f_{22} + \\
&\quad + \gamma f_{24} + 2\alpha f_{31} + 8\delta f_{40} + \delta f_{42}\} \\
p_{20} &= 4\mu^4\alpha\omega\eta/3(1-\nu^2) - 4f_{20}/\eta - 4\mu^2\omega\alpha\sigma^* + \\
&\quad + \frac{\omega}{\eta}\{(1+\delta)f_{11} + 9\gamma f_{13} + 8\beta f_{22} + f_{31} + 9\gamma f_{33} + \delta f_{51}\} \\
p_{02} &= 4\beta\omega\eta/3(1-\nu^2) + \frac{\omega}{\eta}\{(1+\gamma)f_{11} + f_{13} + \gamma f_{15} + 8\alpha f_{22} + 9\delta f_{31} + 9\delta f_{33}\} \\
p_{13} &= (\mu^2+9)^2\gamma\omega\eta/12(1-\nu^2) - f_{13}/\eta - \mu^2\omega\gamma\sigma^* + \\
&\quad + \frac{\omega}{\eta}\{2f_{02} + 8f_{04} + 18\gamma f_{06} + 2\beta f_{11} + 18\alpha f_{13} + 2\beta f_{15} + 18\gamma f_{20} + \\
&\quad + 4(1+4\delta)f_{22} + (1+25\delta)f_{24} + 18\alpha f_{33} + 25\delta f_{42} + 16\delta f_{44}\}
\end{aligned}\right\} \tag{21}$$

and

$$\left.\begin{aligned}
p_{31} &= (9\mu^2+1)^2\delta\omega\eta/12(1-\nu^2) - 9f_{31}/\eta - 9\mu^2\omega\delta\sigma^* + \\
&\quad + \frac{\omega}{\eta}\{18\delta f_{02} + 2\alpha f_{11} + 2f_{20} + 4(1+4\gamma)f_{22} + 25\gamma f_{24} + 18\beta f_{31} + \\
&\quad + 18\beta f_{33} + 8f_{40} + (1+25\gamma)f_{42} + 16\gamma f_{44} + 2\alpha f_{51} + 18\delta f_{60}\}.
\end{aligned}\right\}$$

For any given solution (α, β, γ, δ, ω, η, μ) corresponding to a specific σ^* or e^*, the derived solution is exact if this pressure system is assumed to have been present throughout the loading-up process. The pressure system, which is fictitious, is different for each point on the post-buckled characteristic but for each such point a measure of the optimum selection of the modal parameters (α, β, γ, etc.) is furnished by the proportion of the total stored energy U which derives from $\overline{W}$.

The five pressure coefficients in equation (21) are, or should be, all zero and their vanishing corresponds to the stationary property of U (or for dead-weight loading $U-W$) with respect to the amplitudes ξ, α, β, γ, δ respectively.

Thus $p_{20} = 0$ implies $\partial U/\partial\alpha = 0$ for strain-increment loading. Residues in these p's indicate insufficient progress in the minimizing procedure.

The pressure, however, is not zero over the entire surface, but is merely orthogonal to $w(x, y)$. The thirty component pressures which survive are also of interest, and will be discussed below.

5.1. *Root-Mean Constraint Pressure.*

The constraint pressure over the curved surface of the cylinder is periodic and consists of a number of superposed pressures of the form

$$p = p_{mn}\cos(m\pi x/\lambda_x)\cos(n\pi y/\lambda_y). \tag{22}$$

The root-mean-square pressure $\bar{p}$ is defined by

$$(\bar{p})^2 = \frac{1}{2\pi RL}\int_0^L \int_0^{2\pi R} (p)^2 dx\, dy$$

$$= \frac{1}{2\pi RL}\int_0^L \int_0^{2\pi R} \Sigma\,(p_{mn})^2 \cos^2(m\pi x/\lambda_x)\cos^2(n\pi y/\lambda_y) dx\, dy$$

or

$$\bar{p} = \{\Sigma\,(p_{mn})^2 K\}^{1/2}, \tag{23}$$

where

$K = \frac{1}{4}$ if neither m or n is zero

$K = \frac{1}{2}$ if one of them is zero.

The coefficients p_{mn} which have the values other than zero are:

$$\left.\begin{aligned}
p_{04} &= \frac{4\omega}{\eta}\{\gamma f_{11} + f_{13} + f_{15} + 8\alpha f_{24} + 9\delta f_{33}\}\\
p_{06} &= \frac{9\omega}{\eta}\{\gamma f_{13} + f_{15}\}\\
p_{08} &= 16\omega\gamma f_{15}/\eta\\
p_{15} &= -f_{15}/\eta + \frac{2\omega}{\eta}\left\{\gamma f_{02} + 4f_{04} + 9f_{06} + \beta f_{13} + 25\alpha f_{15} + 8\gamma f_{22} + \right.\\
&\quad \left. + \frac{9+49\delta}{2} f_{24} + 32\delta f_{44}\right\}\\
p_{17} &= \frac{\omega}{\eta}\{8\gamma f_{04} + 18 f_{06} + 2\beta f_{15} + 25\gamma f_{24}\}\\
p_{19} &= 18\omega\gamma f_{06}/\eta\\
p_{22} &= -4f_{22}/\eta + \frac{4\omega}{\eta}\{4\alpha f_{02} + (\gamma+\delta) f_{11} + (1+4\delta) f_{13} + 4\gamma f_{15} + 4\beta f_{20} +\\
&\quad + 2\beta f_{24} + (1+4\gamma) f_{31} + 2\alpha f_{42} + 4\delta f_{51}\}\\
p_{24} &= -4f_{24}/\eta + \frac{\omega}{\eta}\{64\alpha f_{04} + \gamma f_{11} + (1+25\delta) f_{13} + (9+49\delta) f_{15} + 8\beta f_{22} +\\
&\quad + 25\gamma f_{31} + 9 f_{33} + 32\alpha f_{44}\}\\
p_{26} &= \frac{4\omega}{\eta}\{36\alpha f_{06} + (1+16\delta) f_{15} + 2\beta f_{24} + 9\gamma f_{33}\}\\
p_{28} &= \omega\gamma f_{15}/\eta\\
p_{33} &= -9f_{33}/\eta + \frac{9\omega}{\eta}\{2\delta f_{02} + 8\delta f_{04} + 2\alpha f_{13} + 2\gamma f_{20} + f_{24} + 2\beta f_{31} +\\
&\quad + 8\gamma f_{40} + f_{42}\}
\end{aligned}\right\} \tag{24}$$

$$p_{35} = \frac{\omega}{\eta}\{72\delta f_{04} + 162\delta f_{06} + 50\alpha f_{15} + 4\gamma f_{22} + f_{24} + 18\beta f_{33} +$$
$$+ 49\gamma f_{42} + 16 f_{44}\}$$

$$p_{37} = \frac{\omega}{\eta}\{162\delta f_{06} + \gamma f_{24} + 64\gamma f_{44}\}$$

$$p_{40} = -16 f_{40}/\eta + \frac{4\omega}{\eta}\{\delta f_{11} + f_{31} + 9\gamma f_{33} + 8\beta f_{42} + f_{51}\}$$

$$p_{42} = -16 f_{42}/\eta + \frac{\omega}{\eta}\{\delta f_{11} + 25\delta f_{13} + 8\alpha f_{22} + (1+25\gamma) f_{31} + 9 f_{33} +$$
$$+ 64\beta f_{40} + 32\beta f_{44} + (9+49\gamma) f_{51}\}$$

$$p_{44} = -16 f_{44}/\eta + \frac{16\omega}{\eta}\{\delta f_{13} + 4\delta f_{15} + 2\alpha f_{24} + \gamma f_{31} + 2\beta f_{42} + 4\gamma f_{51}\}$$

$$p_{46} = \frac{\omega}{\eta}\{49\delta f_{15} + 9\gamma f_{33} + 32\beta f_{44}\}$$

$$p_{51} = -25 f_{51}/\eta + \frac{\omega}{\eta}\{2\delta f_{20} + 16\delta f_{22} + 2\alpha f_{31} + 8 f_{40} + (9+49\gamma) f_{42} +$$
$$+ 64\gamma f_{44} + 50\beta f_{51} + 18 f_{60}\}$$

$$p_{53} = \frac{\omega}{\eta}\{4\delta f_{22} + 49\delta f_{24} + 18\alpha f_{33} + 72\gamma f_{40} + f_{42} + 16 f_{44} +$$
$$+ 50\beta f_{51} + 162\gamma f_{60}\}$$

$$p_{55} = \frac{25\omega}{\eta}\{\delta f_{24} + \gamma f_{42}\}$$

$$p_{57} = 16\omega\gamma f_{44}/\eta$$

$$p_{60} = -36 f_{60}/\eta + \frac{9\omega}{\eta}\{\delta f_{31} + f_{51}\}$$

$$p_{62} = \frac{4\omega}{\eta}\{9\delta f_{33} + 2\alpha f_{42} + (1+16\gamma) f_{51} + 36\beta f_{60}\}$$

$$p_{64} = \frac{\omega}{\eta}\{9\delta f_{33} + 32\alpha f_{44} + 49\gamma f_{51}\}$$

$$p_{71} = \frac{\omega}{\eta}\{8\delta f_{40} + 25\delta f_{42} + 2\alpha f_{51} + 18 f_{60}\}$$

$$p_{73} = \frac{\omega}{\eta}\{\delta f_{42} + 64\delta f_{44} + 162\gamma f_{60}\}$$

$$p_{75} = 16\omega\delta f_{44}/\eta$$

$$p_{80} = 16\omega\delta f_{51}/\eta$$

$$p_{82} = \omega\delta f_{51}/\eta \text{ and}$$

$$p_{91} = 18\omega\delta f_{60}/\eta .$$

(24)
continued

The root-mean constraint pressure rises steadily as the mean axial strain increases. Typical values of $\bar{p}$ (at $e^* = 1$) are $0{\cdot}204$ for the mode w of equation (10) and $0{\cdot}315$ for Kempner's case.

The root-mean constraint pressure is an index only of the lack of completeness of the solution. The individual pressure coefficients influence the deflection of the cylinder, but those associated with higher-frequency products of $\cos(m\pi x/\lambda_x)\cos(n\pi y/\lambda_y)$ are, for the same amplitude, far less influential than those of lower frequency, for the bending produced is reduced.

For Kempner's case, e^* being taken equal to 1, the largest pressure coefficients are, with values

$$p_{22}(0{\cdot}497),\ p_{31}(-0{\cdot}366),\ p_{40}(0{\cdot}262);\ p_{13}(0{\cdot}213) \text{ and } p_{42}(0{\cdot}0895).$$

For the mode w of equation (10), the corresponding largest pressure coefficients are

$p_{22}(0{\cdot}250)$, $p_{51}(0{\cdot}178)$, $p_{15}(-0{\cdot}132)$, $p_{53}(-0{\cdot}119)$, $p_{40}(-0{\cdot}111)$ and $p_{24}(-0{\cdot}107)$

p_{31} and p_{13} are, of course, negligibly small.

An examination of the constraint pressure system over the range e^* varying from $0{\cdot}3$ to $1{\cdot}2$ shows that the following eight pressure coefficients always include the six largest pressure components for e^* in that range:

$$p_{15},\ p_{22},\ p_{24},\ p_{33},\ p_{40},\ p_{42},\ p_{51} \text{ and } p_{53}.$$

The pressure systems are plotted, over the area covered by the mode diagram in Fig. 5, for both Kempner's case and the present paper in Figs. 8 and 9 respectively.

Examination of the pressure distributions and their correlation with the modal pattern shows that for the Kempner case, the pressures are highest at the extremes of the deflections, and at the saddle point between hills and dales. These are regions of considerable bending where inaccuracies of the mode shape are most important. By contrast, these important zones are all associated with low pressure levels using the extended mode w of equation (10) and indicate that minor corrections only are to be sought in the mode pattern.

To improve the solution still further, an improved mode may be calculated from equation (8) using expressions (22) for p, (11) for F and (10) for w on the right-hand side. This shows that if the mode is to be improved, it should include those terms whose periodicities in x and y correspond with those of the pressures enumerated above. The influence of all, or some of these further perturbing terms is likely to be far less marked than the inclusion of the two additional terms to Kempner's mode, with the possible exception of the (2, 2) term.

6. *Conclusions.*

A significant reduction in the post-buckled stress levels for a given strain is achieved using a full perturbation of the linear solution to this problem. By direct calculation of the system of pressures necessary to maintain the mode, it is clear that only small improvements in the stress-strain characteristic can be expected from further analysis and that the 'true' solution of the von Karman large-deflection system for the given problem is not far below the characteristic given.

No importance is attached to advanced post-buckled behaviour, which, in this ideal investigation, is of little significance, but it is interesting to note that the post-buckled stiffness of the cylinder in the immediate post-buckled condition (dead-weight-loading case) is about 10% of the initial unbuckled value compared with a predicted $16{\cdot}5\%$ in Kempner's case.

Specific values for buckling stresses and strains are given in Tables 1 and 2 for the extreme loading conditions.

LIST OF SYMBOLS

x	Cartesian co-ordinate measured along a generator
y	Cartesian co-ordinate measured around cylinder
z	Cartesian co-ordinate measured radially inward

see Fig. 1

σ_x, σ_y	Direct stresses parallel to axes Ox, Oy respectively
τ_{xy}	Shear stress in the tangent plane
F	Airy stress function
ϵ_x, ϵ_y	Direct strains parallel to axes Ox, Oy respectively
γ_{xy}	Shear strain in tangent plane
u, v, w	Displacements parallel to axes Ox, Oy and Oz
E	Young's modulus
ν	Poisson's ratio
R	Radius of cylinder
p	Radially inward pressure
t	Thickness of cylinder
D	Flexural rigidity of cylinder $= \frac{1}{12} Et^3(1-\nu^2)^{-1}$
λ_x, λ_y	Wavelengths in x, y direction associated with mode $w(x, y)$
ξ, α, β, γ, δ, ϵ	Non-dimensional displacement parameters
μ	$= \lambda_y/\lambda_x$
η	$= \pi^2 Rt/\lambda_y^2$
ω	$= \xi\eta$
f_{mn}	Coefficients occurring in F
σ, e	Mean axial stress and strain respectively
U, U_1, U_2	Total, bending and extensional strain-energy functions
σ^*	Reduced mean axial stress $= \sigma R/Et$
e^*	Reduced mean axial strain $= eR/t$
W	Potential energy of loading device
$\overline{W}$	Work done by constraints
p_{mn}	Pressure coefficients

REFERENCES

No.	*Author(s)*	*Title, etc.*
1	Th. von Karman and H. S. Tsien ..	The buckling of thin cylindrical shells under axial compression. *J. Ae. Sci.*, Vol. 8, No. 8, p. 303. June, 1941.
2	D. M. A. Leggett and R. P. N. Jones..	The behaviour of a cylindrical shell under axial compression when the buckling load has been exceeded. A.R.C. R. & M. 2190. August, 1942.
3	Herman F. Michielsen	The behaviour of thin cylindrical shells after buckling under axial compression. *J. Ae. Sci.*, Vol. 15, No. 12, p. 738. December, 1948.
4	Joseph Kempner	Post-buckling behaviour of axially compressed circular cylindrical shells. *J. Ae. Sci.*, Vol. 21, No. 5, p. 329. May, 1954.
5	W. F. Thielmann	New developments in the non-linear theories of the buckling of thin cylindrical shells. Proc. Durand Centennial Conf. Aeronautics and Astronautics, pp. 76 to 119. Pergamon. 1960.
6	H. S. Tsien	Lower buckling load in the non-linear buckling theory of thin shells. *Quart. App. Math.*, Vol. 5, p. 236. 1947.
7	H. H. Rosenbrock	An automatic method for finding the greatest or least value of a function. *Computer Journal*, Vol. 3, No. 3, p. 175. October, 1960.

TABLE 1

Rigid-Loading Conditions

	This paper	Kempner	$\frac{\text{Kempner}}{\text{This paper}}$
Upper limit of buckling strain e^*	0·336	0·360	1·071
Lower limit of buckling strain e^*	0·287	0·306	
Energy jump to buckle at lower limit . . .		0·0149	
Proportional energy increase to jump . . .		0·0159	

TABLE 2

Dead-Weight-Loading Conditions

	This paper	Kempner	$\frac{\text{Kempner}}{\text{This paper}}$
Upper limit of buckling stress σ^*	0·1861	0·2240	1·204
Lower limit of buckling stress σ^*	0·1496	0·1824	1·219
Energy jump to buckle at lower limit . . .	0·0319	0·0352	
Proportional energy increase to jump . . .	1·571	0·961	

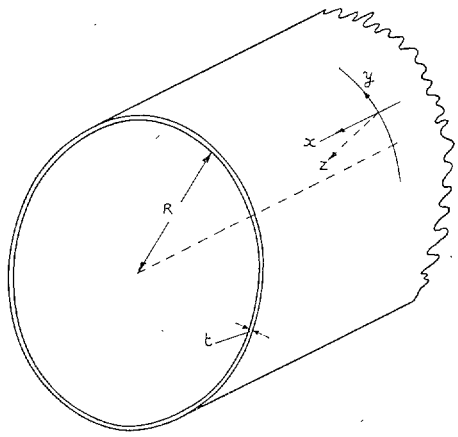

FIG. 1. Cylinder and co-ordinate system.

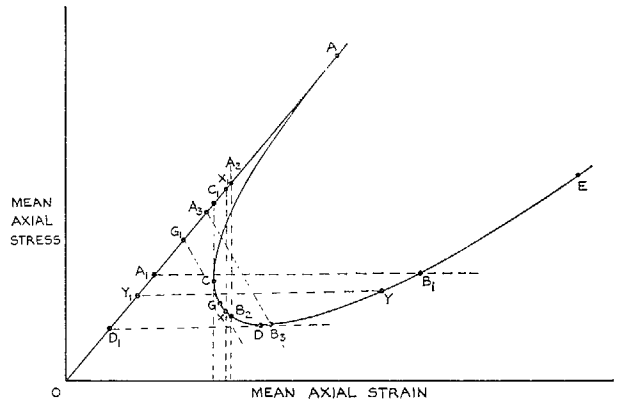

FIG. 2a. Stress-strain diagram for cylinder.

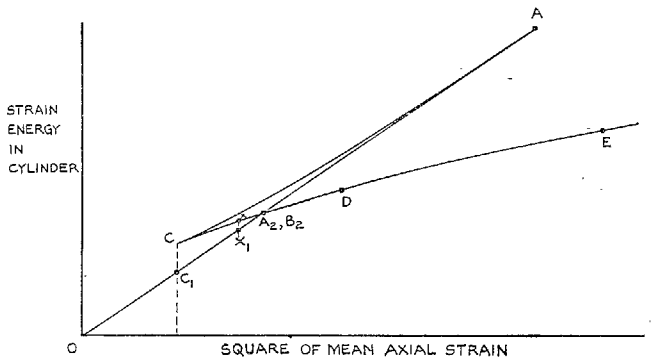

FIG. 2b. Strain-energy diagram for cylinder.

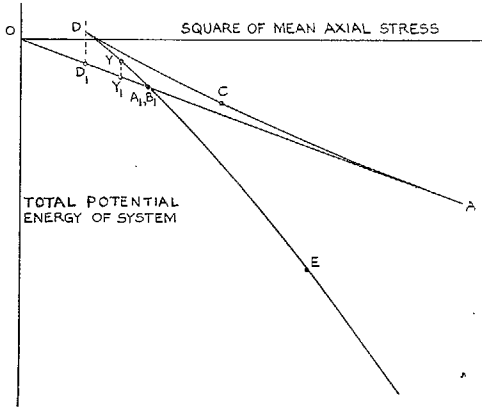

FIG. 2c. Total-potential-energy diagram for dead-weight-loading conditions.

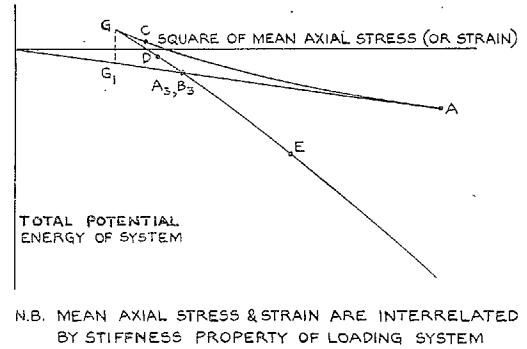

N.B. MEAN AXIAL STRESS & STRAIN ARE INTERRELATED BY STIFFNESS PROPERTY OF LOADING SYSTEM

FIG. 2d. Total-potential-energy diagram for general spring loading of cylinder.

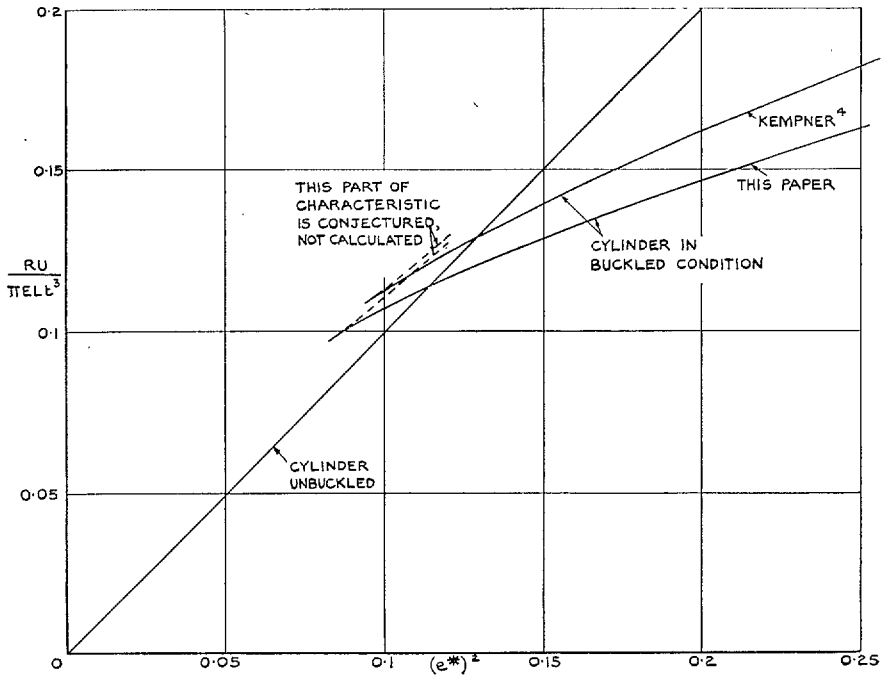

FIG. 3. Variation of strain energy in cylinder for rigid-machine-loading conditions.

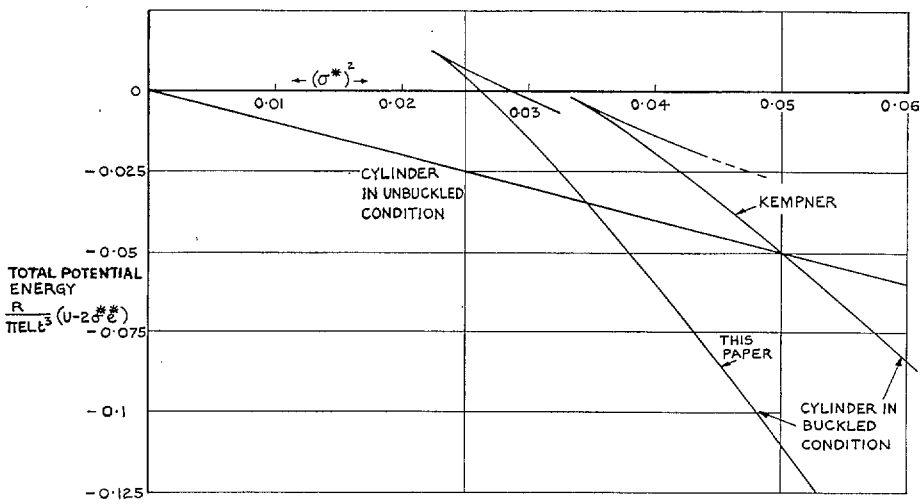

FIG. 4. Variation of total potential energy for dead-weight-loading conditions.

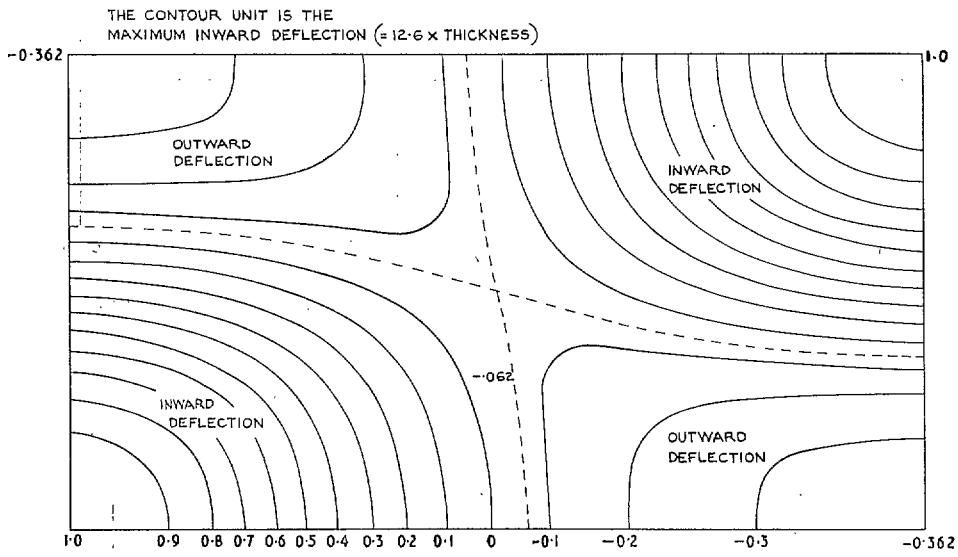

FIG. 5. Modal pattern for $eR/t = 1$ showing contours of alternate hills and dales.

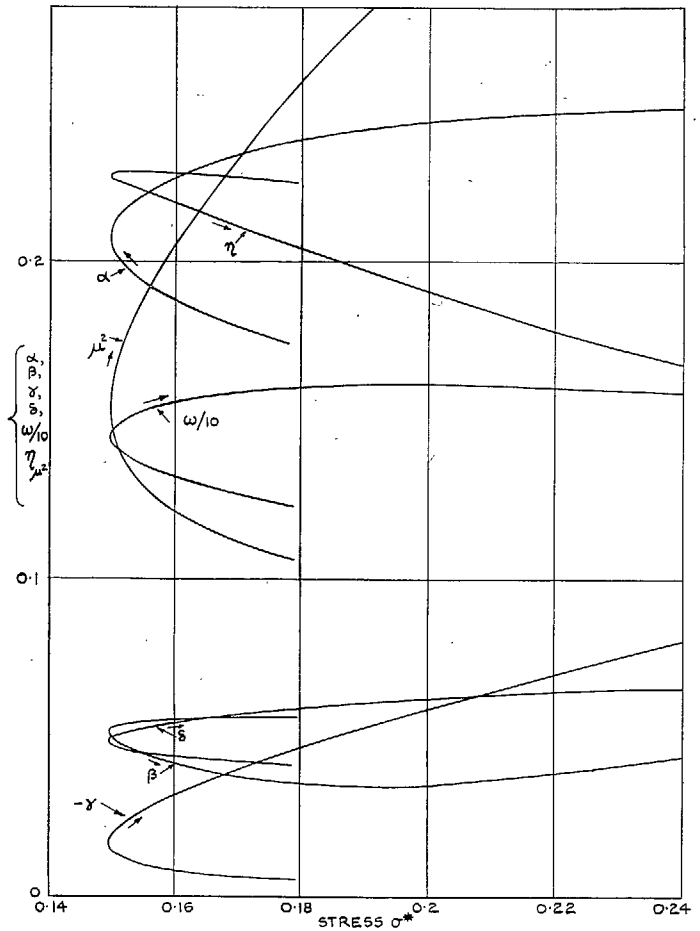

FIG. 6. Variation of modal parameters with mean applied axial stress in the region of minimum post-buckled stress.

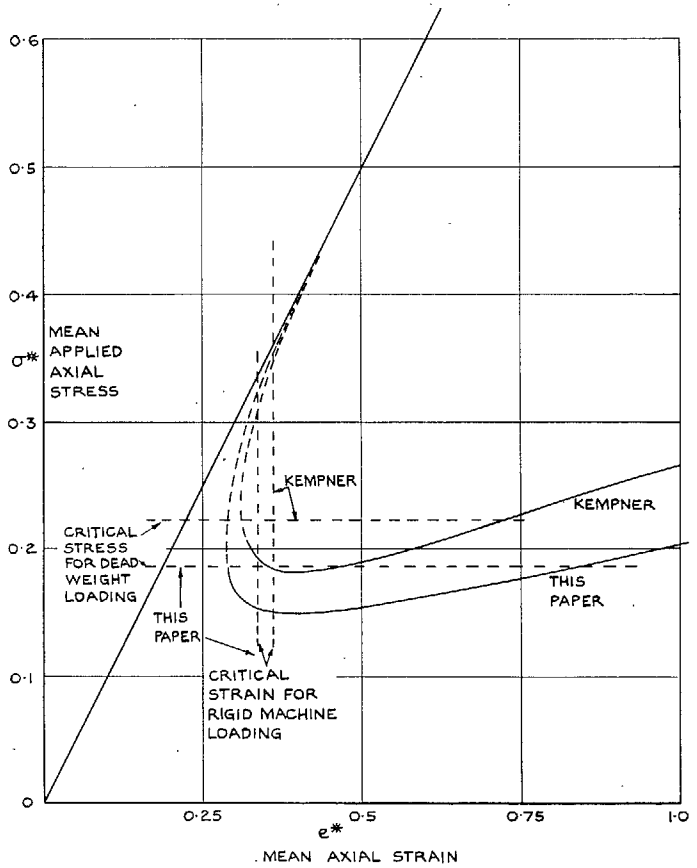

FIG. 7. Stress-strain diagram for the buckled cylinder.

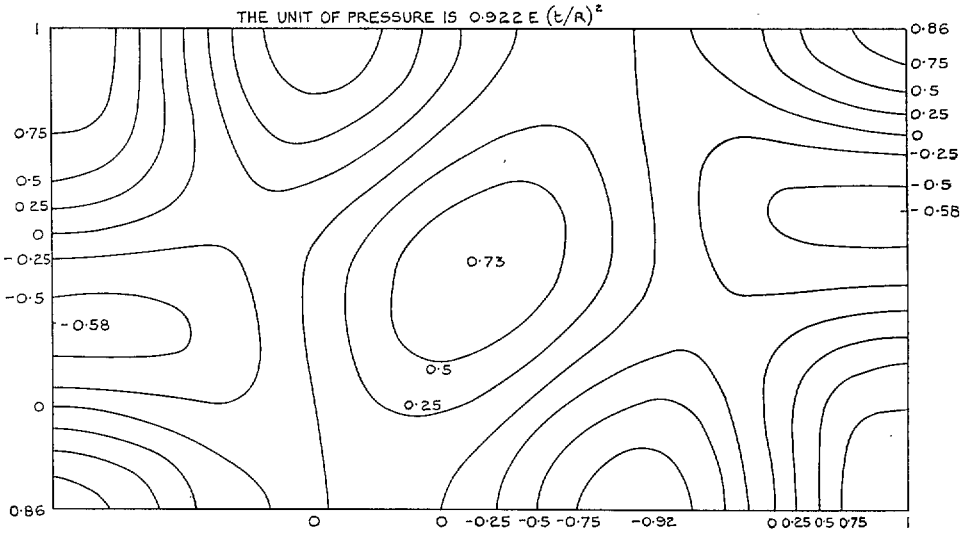

FIG. 8. Pressure contours over region of Fig. 5 for Kempner's mode.

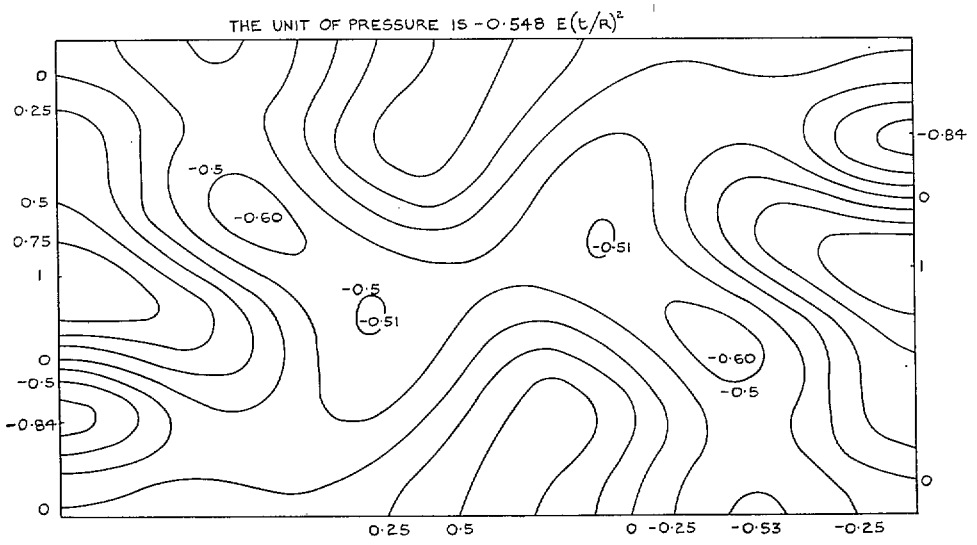

FIG. 9. Pressure contours over region of Fig. 5 for extended mode.

(89024) Wt. 65/1418 K.5 5/64 Hw.

Publications of the Aeronautical Research Council

ANNUAL TECHNICAL REPORTS OF THE AERONAUTICAL RESEARCH COUNCIL (BOUND VOLUMES)

1942 Vol. I. Aero and Hydrodynamics, Aerofoils, Airscrews, Engines. 75*s.* (post 2*s.* 9*d.*)
Vol. II. Noise, Parachutes, Stability and Control, Structures, Vibration, Wind Tunnels. 47*s.* 6*d.* (post 2*s.* 3*d.*)

1943 Vol. I. Aerodynamics, Aerofoils, Airscrews. 80*s.* (post 2*s.* 6*d.*)
Vol. II. Engines, Flutter, Materials, Parachutes, Performance, Stability and Control, Structures. 90*s.* (post 2*s.* 9*d.*)

1944 Vol. I. Aero and Hydrodynamics, Aerofoils, Aircraft, Airscrews, Controls. 84*s.* (post 3*s.*)
Vol. II. Flutter and Vibration, Materials, Miscellaneous, Navigation, Parachutes, Performance, Plates and Panels, Stability, Structures, Test Equipment, Wind Tunnels. 84*s.* (post 3*s.*)

1945 Vol. I. Aero and Hydrodynamics, Aerofoils. 130*s.* (post 3*s.* 6*d.*)
Vol. II. Aircraft, Airscrews, Controls. 130*s.* (post 3*s.* 6*d.*)
Vol. III. Flutter and Vibration, Instruments, Miscellaneous, Parachutes, Plates and Panels, Propulsion. 130*s.* (post 3*s.* 3*d.*)
Vol. IV. Stability, Structures, Wind Tunnels, Wind Tunnel Technique. 130*s.* (post 3*s.* 3*d.*)

1946 Vol. I. Accidents, Aerodynamics, Aerofoils and Hydrofoils. 168*s.* (post 3*s.* 9*d.*)
Vol. II. Airscrews, Cabin Cooling, Chemical Hazards, Controls, Flames, Flutter, Helicopters, Instruments and Instrumentation, Interference, Jets, Miscellaneous, Parachutes. 168*s.* (post 3*s.* 3*d.*)
Vol. III. Performance, Propulsion, Seaplanes, Stability, Structures, Wind Tunnels. 168*s.* (post 3*s.* 6*d.*)

1947 Vol. I. Aerodynamics, Aerofoils, Aircraft. 168*s.* (post 3*s.* 9*d.*)
Vol. II. Airscrews and Rotors, Controls, Flutter, Materials, Miscellaneous, Parachutes, Propulsion, Seaplanes, Stability, Structures, Take-off and Landing. 168*s.* (post 3*s.* 9*d.*)

1948 Vol. I. Aerodynamics, Aerofoils, Aircraft, Airscrews, Controls, Flutter and Vibration, Helicopters, Instruments, Propulsion, Seaplane, Stability, Structures, Wind Tunnels. 130*s.* (post 3*s.* 3*d.*)
Vol. II. Aerodynamics, Aerofoils, Aircraft, Airscrews, Controls, Flutter and Vibration, Helicopters, Instruments, Propulsion, Seaplane, Stability, Structures, Wind Tunnels. 110*s.* (post 3*s.* 3*d.*)

Special Volumes

Vol. I. Aero and Hydrodynamics, Aerofoils, Controls, Flutter, Kites, Parachutes, Performance, Propulsion, Stability. 126*s.* (post 3*s.*)
Vol. II. Aero and Hydrodynamics, Aerofoils, Airscrews, Controls, Flutter, Materials, Miscellaneous, Parachutes, Propulsion, Stability, Structures. 147*s.* (post 3*s.*)
Vol. III. Aero and Hydrodynamics, Aerofoils, Airscrews, Controls, Flutter, Kites, Miscellaneous, Parachutes, Propulsion, Seaplanes, Stability, Structures, Test Equipment. 189*s.* (post 3*s.* 9*d.*)

Reviews of the Aeronautical Research Council

1939–48 3*s.* (post 6*d.*) 1949–54 5*s.* (post 5*d.*)

Index to all Reports and Memoranda published in the Annual Technical Reports

1909–1947 R. & M. 2600 (out of print)

Indexes to the Reports and Memoranda of the Aeronautical Research Council

Between Nos. 2351–2449	R. & M. No. 2450 2*s.* (post 3*d.*)
Between Nos. 2451–2549	R. & M. No. 2550 2*s.* 6*d.* (post 3*d.*)
Between Nos. 2551–2649	R. & M. No. 2650 2*s.* 6*d.* (post 3*d.*)
Between Nos. 2651–2749	R. & M. No. 2750 2*s.* 6*d.* (post 3*d.*)
Between Nos. 2751–2849	R. & M. No. 2850 2*s.* 6*d.* (post 3*d.*)
Between Nos. 2851–2949	R. & M. No. 2950 3*s.* (post 3*d.*)
Between Nos. 2951–3049	R. & M. No. 3050 3*s.* 6*d.* (post 3*d.*)
Between Nos. 3051–3149	R. & M. No. 3150 3*s.* 6*d.* (post 3*d.*)

HER MAJESTY'S STATIONERY OFFICE

from the addresses overleaf

Printed and published by
HER MAJESTY'S STATIONERY OFFICE

To be purchased from
York House, Kingsway, London W.C.2
423 Oxford Street, London W.1
13A Castle Street, Edinburgh 2
109 St. Mary Street, Cardiff
39 King Street, Manchester 2
50 Fairfax Street, Bristol 1
35 Smallbrook, Ringway, Birmingham 5
80 Chichester Street, Belfast 1
or through any bookseller

Printed in England

S.O. Code No. 23-3366